LASER INTERFEROMETER GRAVITATIONAL WAVE OBSERVATORY
-LIGO-
CALIFORNIA INSTITUTE OF TECHNOLOGY
MASSACHUSETTS INSTITUTE OF TECHNOLOGY

Technical Note **LIGO-T040042-00-Z- 00- D** August 2004

MDC frames for S2 burst analysis

I. Yakushin, S. Klimenko and M. Rakhmanov

This is an internal working note
of the LIGO Project.

California Institute of Technology
LIGO Project - MS 18-34
Pasadena CA 91125
Phone (626) 395-2129
Fax (626) 304-9834
E-mail: info@ligo.caltech.edu

Massachusetts Institute of Technology
LIGO Project - MS NW17-161
Cambridge, MA 02139
Phone (617) 253-4824
Fax (617) 253-4824
E-mail: info@ligo.mit.edu

WWW: http://www.ligo.caltech.edu/

Contents

1 Motivation

There are currently several algorithms for burst searches: TFclusters, Slope, Excess Power, WaveBurst, BlockNormal, r-statistics, etc. There is a need for common benchmark tests that would compare algorithms by

- triple coincidence efficiency for various waveforms,
- an ability to reconstruct properties of detected events,
- background event rate.

Some of these algorithms use LDAS and LAL (TFcluster, Slope, WaveBurst), some only use LAL and run under Condor (ExcessPower), some use Matlab (BlockNormal, r-statistics), C++. The only common denominator is that all the ETGs must be able to read frames.

To be able to compare and combine different algorithms, the Mock Data Challenge (MDC) frames with injected signals of various waveforms and strains are produced. Each ETG takes a sum of time series from MDC frames and raw AS_Q data as an input and reports a list of detected triggers and their reconstructed parameters such as central time, duration, central frequency, bandwidth, strain, etc.

2 Implementation

The MDC frames were generated for several injected waveforms for S2 triple coincidence data set. The total livetime is defined by John Zweizig's (version 3) segment list [1]. The v3 segment list contained intervals with unavailable calibration data which caused the failure of some frame-generating LDAS jobs. As a result different MDC sets might have slightly different number of survived time intervals and different number of injected waveforms.

The arrival time of injected signals is randomly chosen in such a way that there is on average 61 seconds between consecutive injections. Our study [2] indicated that more frequent injections can lead to underestimation of the detection efficiency for some algorithms.

The sky position of a source and polarization angle are randomly chosen from a uniform distribution. Beam pattern coefficients and time delays between LHO and LLO sites are computed (for mathematical details see [3] or section below) using Matlab script [4]. Optimal inclination of sources with respect to Earth is assumed.

The frames were generated with the LDAS datacon [4] and compressed by a factor of 50 by using DMTGen tool [5]. The validity of the frames was tested by P. Sutton [6].

Each frame contains 600 seconds filled with zeroes and injection waveforms. There are three ADC channels in each frame: L1:GW, H1:GW, and H2:GW. The dataconAPI function respfilt() was used to convert signals from strain to ADC count. Each waveform

below, except for the black hole merger waveform (BH6), has one polarization. The BH6 waveforms have two polarizations.

3 List of available frames

The following frames were generated to be used for the S2 burst analysis.

3.1 SG10: Sine-gaussian waveforms

The sine-gaussian waveforms are generated in the same way as described in S1 paper [7] with $Q = 9$ and the following frequencies: 100, 153, 235, 361, 554, 849 Hz.

The stregth of the waveforms (in units of strain) is randomly chosen from the following list: 3e-21, 3.93e-21, 5.14e-21, 6.73e-21, 8.81e-21, 1.15e-20, 1.51e-20, 1.98e-20, 2.59e-20, 3.39e-20, 4.44e-20, 5.81e-20, 7.61e-20, 9.96e-20, 1.3e-19, 1.71e-19, 2.23e-19, 2.92e-19, 3.83e-19, 5.01e-19. The total number of injections is 16922. The total number of 600 second frames is 1759 (1055400 seconds, 293 hours). There are approximately 140 injections per each strain-waveform pair.

3.2 GA2: Gaussian waveforms

The waveforms are generated in the same way as described in S1 paper [7] with the waveform duration (τ) taking values 0.1, 0.5, 1.0, 2.5, 4.0, 6.0 ms.

The strength of the waveforms (in units of strain) is randomly chosen from the following list: 4.5e-21, 6.07e-21, 8.19e-21, 1.1e-20, 1.49e-20, 2.01e-20, 2.71e-20, 3.66e-20, 4.93e-20, 6.66e-20, 8.98e-20, 1.21e-19, 1.63e-19, 2.2e-19, 2.97e-19, 4.01e-19, 5.41e-19, 7.3e-19, 9.84e-19, 1.33e-18. The total number of injections is 16540. The total number of 600 second frames is 1698. There are approximately 142 injections per each strain-waveform pair.

3.3 BH6: Black hole merger Lazarus waveforms

The waveforms are described in [8] and they are generated for black hole binaries with masses of 10, 30, 50, 70 and 90 solar masses.

The strength of the waveforms (in units of strain) is randomly chosen from the following list: 6.36e-21, 8.58e-21, 1.16e-20, 1.56e-20, 2.11e-20, 2.84e-20, 3.83e-20, 5.17e-20, 6.98e-20, 9.41e-20, 1.27e-19, 1.71e-19, 2.31e-19, 3.12e-19, 4.2e-19, 5.67e-19, 7.65e-19, 1.03e-18, 1.39e-18, 1.88e-18. The total number of injections is 16980. The total number of 600 second frames is 1698. There are approximately 172 injections per each strain-waveform pair.

3.4 ZM1: Zwerger-Muller and Dimmelmeier-Font-Muller waveforms for supernova collapse

All known (103) ZM and DFM waveforms [9]-[10] are injected. The total number of injections is 16920. The total number of 600 second frames is 1692. The strength of the waveforms is selected depending on the distance to the source. The distance (in units of parsecs) is randomly chosen from the following list: 1000.43, 785.077, 616.086, 483.468, 379.397, 297.73, 233.641, 183.348, 143.881, 112.909, 88.6046, 69.5318, 54.5646, 42.8192, 33.602, 26.3689, 20.6928, 16.2385, 12.743, 10.

3.5 BO2: Ott-Burrows waveforms for supernova collapse

All known (71) Ott-Burrows waveforms [11] are injected. The total number of injections is 16980. The total number of 600 second frames is 1698. For injections of BO2 waveforms the same list of distances to sources as for ZM1 is used.

3.6 Availability of MDC frames

All described MDC frames are available at CIT, some frames are available at LLO, LHO, PSU, UWM and MIT. For more information about the MDC frames, including lists of injections and what frames are available at each site, see [12].

4 Beam pattern coefficients and delays as a function of source sky position and polarization

In this section we describe how, given sky position and polarization, beam pattern coefficients and delays in arrival time are computed for LLO and LHO sites.

4.1 Gravitational wave signal

The metric for gravitational waves is

$$g_{\mu\nu} = \eta_{\mu\nu} + h_{\mu\nu}, \tag{1}$$

where $\eta_{\mu\nu}$ is the Minkowski metric and $h_{\mu\nu}$ is the strain tensor of gravitational waves. In the transverse traceless (TT) coordinates the strain tensor takes the form:

$$h_{\mu\nu} = \begin{pmatrix} 0 & & & \\ & h_+ & h_\times & \\ & h_\times & -h_+ & \\ & & & 0 \end{pmatrix}, \tag{2}$$

where h_+ and $h_\times$ correspond to two different polarizations of the gravitational wave. For most of our analysis time can be regarded as a fixed dimension and no time-dependent

coordinate transformations will be necessary. We therefore can safely neglect the time components of the 4-dimensional tensors and consider only their spatial (3-dimensional) parts. In this case, the gravitational wave strain tensor can be represented by a sum of two 3-dimensional matrices:

$$\mathbf{h} = h_+ \, \mathbf{m} + h_\times \, \mathbf{n}. \tag{3}$$

where $\mathbf{m}$ is a traceless and $\mathbf{n}$ is a transverse unit tensor

$$\mathbf{m} = \begin{pmatrix} 1 & 0 & 0 \\ 0 & -1 & 0 \\ 0 & 0 & 0 \end{pmatrix}, \qquad \mathbf{n} = \begin{pmatrix} 0 & 1 & 0 \\ 1 & 0 & 0 \\ 0 & 0 & 0 \end{pmatrix}. \tag{4}$$

A laser interferometer defines its own coordinate system so that x and y axes run along the two interferometer arms, and the origin is at the beam-splitter. In general, these coordinates are oriented differently from the TT-coordinates of the gravitational wave introduced above. The two coordinate systems can be related by rotational transformation

$$\mathbf{x}' = \mathbf{R}^T \, \mathbf{x}, \tag{5}$$

where $\mathbf{x}$ are the coordinates associated with the gravitational wave and $\mathbf{x}'$ and are the coordinates associated with the detector.

The rotational transformation induces the transformation of the metric. The strain tensor in the detector frame, $\mathbf{h}'$, can be found from the original tensor $\mathbf{h}$ by means of the induced transformation:

$$\mathbf{h}' = \mathbf{R}^T \mathbf{h} \, \mathbf{R}. \tag{6}$$

A laser interferometer generates signal from the difference between the length of the x and y arms, and therefore is proportional to

$$V = \frac{1}{2} \, \mathrm{Tr} \left\{ \mathbf{m} \, \mathbf{h}' \right\}. \tag{7}$$

Such a signal is a sum of two parts each originating from an independent polarization:

$$V = F_+ \, h_+ + F_\times \, h_\times. \tag{8}$$

The antenna patterns F_+ and $F_\times$ depend on the orientation of the detector with respect to the source and its polarization axes:

$$F_+ = \frac{1}{2} \, \mathrm{Tr} \left\{ \mathbf{m} \, \mathbf{R}^T \mathbf{m} \, \mathbf{R} \right\}, \tag{9}$$

$$F_\times = \frac{1}{2} \, \mathrm{Tr} \left\{ \mathbf{m} \, \mathbf{R}^T \mathbf{n} \, \mathbf{R} \right\}. \tag{10}$$

The normalization factors 2^{-1} ensure that the maximum value for the antenna patterns is equal to 1.

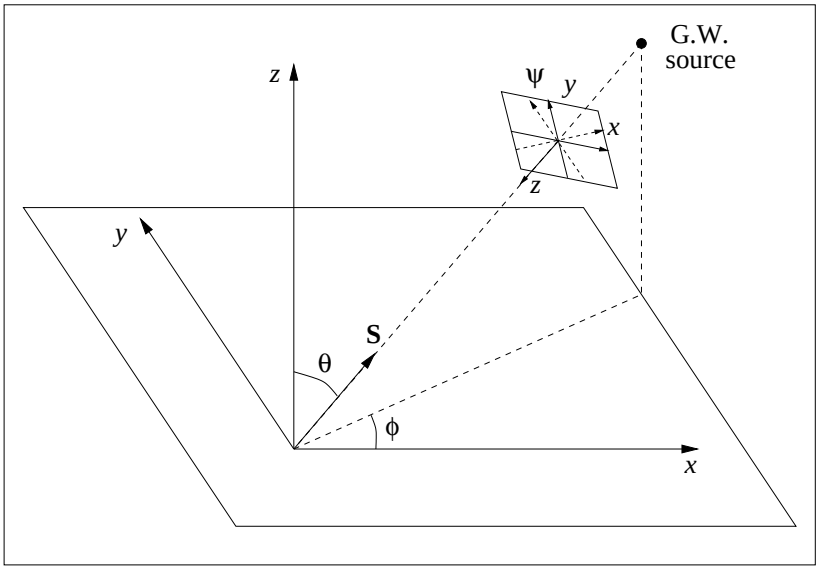

4.2 Generation of Random Angles and Arrival Times

The position of the source on the sky is givn by ϕ, θ) and its polarization by ψ. These angles are produced by a random number generator:

$$\phi = 2\pi \ \mathrm{rand}(1), \tag{11}$$

$$\theta = \arccos[1 - 2 \ \mathrm{rand}(1)], \tag{12}$$

$$\psi = 2\pi \ \mathrm{rand}(1). \tag{13}$$

The peculiar form of random generation for θ is to ensure proper density of random points on a sphere.

Then these angles were used for defining several rotational transformations.

Transformation from Hanford frame to the G.W. frame

$$\mathbf{U} = \mathbf{R}_z(\psi) \ \mathbf{R}_y(\theta - \pi) \ \mathbf{R}_z(\phi). \tag{14}$$

Transformation from Livingston frame to Hanford frame

$$\mathbf{V} = \mathbf{R}_z(-\beta_1) \ \mathbf{R}_y(2\alpha) \ \mathbf{R}_z(\beta_2). \tag{15}$$

Complete rotational transformation

$$\mathbf{R}_1 = \mathbf{U}, \tag{16}$$

$$\mathbf{R}_2 = \mathbf{U} \ \mathbf{V} \tag{17}$$

Antenna patterns (1 for Hanford and 2 for Livingston):

$$F_{+1} = \frac{1}{2} \ \mathrm{Tr}\left\{\mathbf{m} \, \mathbf{R}_1^T \mathbf{m} \, \mathbf{R}_1\right\}, \tag{18}$$

$$F_{+2} = \frac{1}{2}\,\mathrm{Tr}\left\{\mathbf{m}\,\mathbf{R}_2^T\mathbf{m}\,\mathbf{R}_2\right\}, \tag{19}$$

$$F_{\times 1} = \frac{1}{2}\,\mathrm{Tr}\left\{\mathbf{m}\,\mathbf{R}_1^T\mathbf{n}\,\mathbf{R}_1\right\}, \tag{20}$$

$$F_{\times 2} = \frac{1}{2}\,\mathrm{Tr}\left\{\mathbf{m}\,\mathbf{R}_2^T\mathbf{n}\,\mathbf{R}_2\right\}. \tag{21}$$

Define two vectors: $\vec{p}$ and $\vec{S}$. Vector $\vec{p}$ is connecting the two sites (Fig. 2) and vector the unit vector pointing to the souce of G.W. defined at the Hanford site:

$$S_x = \sin\theta\,\cos\phi, \tag{22}$$

$$S_y = \sin\theta\,\sin\phi, \tag{23}$$

$$S_z = \cos\theta. \tag{24}$$

Then the delay of G.W. arrival at Livingston with respect to Hanford

$$\tau = \frac{1}{c}\,\vec{p}\cdot\vec{S} \tag{25}$$

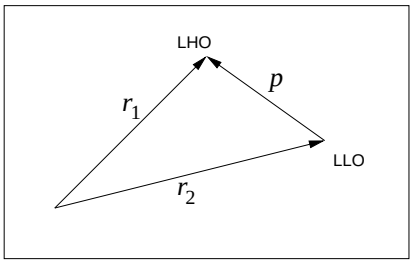

In the simulation this delay time is offset by 20 msec, changed to nanosec, and then rounded to the nearest integer nanosecond:

$$\tau = \tau + 0.02, \tag{26}$$

$$\tau = \tau \times 10^9, \tag{27}$$

$$\tau = \mathrm{round}(\tau). \tag{28}$$

The a random arrival time is generated for the G.W. wave:

$$t = (1/32)\,[2\,\mathrm{rand}(1) - 1], \tag{29}$$

$$t = t \times 10^9, \tag{30}$$

$$t = \mathrm{round}(t) \tag{31}$$

The numbers stored are:

$$\phi, \quad \theta, \quad \psi, \quad F_{+1}, \quad F_{+2}, \quad F_{\times 1}, \quad F_{\times 2}, \quad t, \quad \tau \tag{32}$$

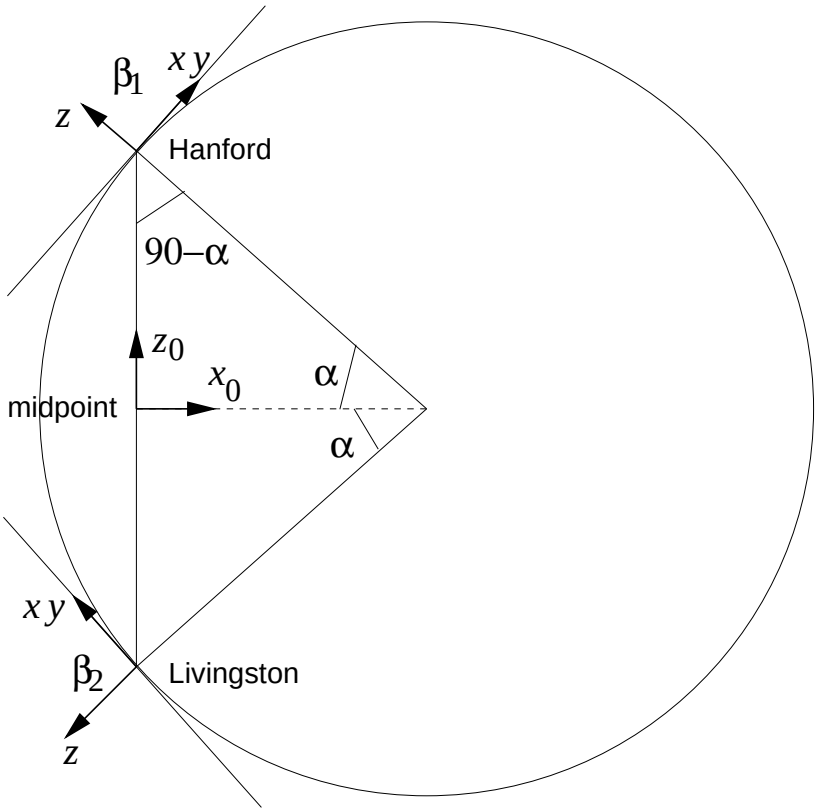

4.3 Orientation of the LIGO Hanford and Livingston interferometers in the Earth tangential planes

α is the angle between the z axes of the detectors, and β_1 and β_2 are the angles of x-axis of the detectors and the vector $\vec{p}$:

$$\alpha = 13.612^0, \tag{33}$$

$$\beta_1 = 28.42^0, \tag{34}$$

$$\beta_2 = -61.52^0. \tag{35}$$

References

[1] J. Zweizig. Burst Analysis Segment Lists. `http://www.ligo.caltech.edu/~jzweizig/S2_Data_Quality/Burst_Segments`.

[2] I. Yakushin. Are we underestimating the detection efficiency on MDC frames? `http://www.ligo-la.caltech.edu/~igor/MDC/InjectionFrequency/index.html`.

[3] S. Klimenko and M. Rakhmanov. Angular Correlation of LIGO Hanford and Livingston Interferometers. Technical Report T030215-00-D, UF, 2003.

[4] Software used to produce MDC frames. `http://www.lsc-group.phys.uwm.edu/cgi-bin/cvs/viewcvs.cgi/Igor/burstMDC%/?cvsroot=lscsoft`.

[5] J. Zweizig. DMTGen. `http://www.ligo.caltech.edu/~jzweizig/dmt/generator/DMTGen.html`.

[6] P. Sutton. MDC Frame Verification in the S2 Bursts Search (Preliminary report). `http://ligo.caltech.edu/~psutton/DCC_Documents/Sutton_T040082-00.pdf`.

[7] LSC collaboration. First upper limits from LIGO on gravitational wave bursts. gr-qc/0312056v4.

[8] J. Baker, M. Campanelli, C.O. Lousto, and R. Takahashi. Modeling gravitational radiation from coalescing binary black holes. astro-ph/0202469.

[9] T. Zwerger and E. Muller. Dynamics and gravitational wave signature of axisymmetric rotational core collapse. *Astron. Astrophys.*, 320:209–227, 1997.

[10] H. Dimmelmeier, J. A. Font, and E. Muller. Relativistic simulations of rotational core collapse. ii. collapse dynamics and gravitational radiation. *Astron. Astrophys.*, 393:523–542, 2002.

[11] Christian D. Ott, Adam Burrows, Eli Livne, and Rolf Walder. Gravitational waves from axisymmetric, rotational stellar core collapse. *Astrophys.J*, 600:834–864, 2004.

[12] I. Yakushin, S. Klimenko, and M. Rakhmanov. Burst MDC frames. `http://www.ligo-la.caltech.edu/~igor/MDC`.